Thermo-mechanical problems: Eulerian-Lagrangian approach within Kratos-GiD framework

P. Ryzhakov, R. Rossi, E. Oñate

May 12, 2010

Abstract

Fluid-structure interaction and generally coupled problems define the "hot-spots" in the computational mechanics. Resolution of those requires both the tools for modeling/visualization and the efficient solvers. Here we present a combination of GID-pre/post-processor with Kratos-Multi Physics tool.

In particular we present a coupled Eulerian-Lagrangian algorithm for solution of complicated thermo-mechanical problems involving thermo-mechanical interaction between an object (or viscous fluid) and the ambience. In the proposed approach the Lagrangian domain is moving on top of the fixed Eulerian mesh, following the core concept of embedded methods. The mechanical interaction is thus taking place on the Eulerian mesh, separated into real, fictitious, and interface sub-domains by the image of the Lagrangian domain onto Eulerian mesh. This approach permits to enjoy all the advantages of the Lagrangian method with respect to interface definitions, while save the computational effort associated with the re-meshing on a major part of the computational domain, that is treated by the Eulerian formulation.

Using compressible model for the ambience leads to two important advantages. First, it permits consideration of thermal problems without restriction upon temperature gradients (that exists when Boussinesq hypothesis-based solvers are used). On the other hand, compressibility of the ambience eliminates convergence problem of the FSI and permits the application of standard Dirichlet-Neumann coupling. However the results presented here are obtained by using one-way Dirichlet coupling, justified by the physical properties of the constituents in the problem of interest.

From the point of view of pre/post-processing,.our approach has a number of algorithmic peculiarities such as necessity of outputting simultaneously both the Eulerian and Lagrangian meshes as well as possibility of "disabling" parts of the domain. Some of these aspects are successfully tackled with the present version of GiD, while simplification of the implementation of the others still needs to be considered.

1 Formulation

In this section the set of discrete governing equations are presented.

Lagrangian formulation for the fluid Eulerian-Lagrangian algorithms have been proposed for solution of the fluid-structure interaction problem [1], [2]. We extend them to the interaction between the two fluids. The viscous free surface flow will be modeled using the Particle Finite Element Method formulation [3]. [4]. We reproduce here the final discrete system for the incompressible fluid after application of the fractional step technique [5].

$$\mathbf{M}\frac{\tilde{\mathbf{v}}-\bar{\mathbf{v}}_n}{\Delta t}+\nu\mathbf{L}\tilde{\mathbf{v}}+\mathbf{G}\bar{p}_n=\mathbf{F}_{n+\theta} \tag{1}$$

$$\Delta t\mathbf{L}\left(\bar{p}_{n+1}-\bar{p}_n\right)+\mathbf{S}\bar{p}_{n+1}=\mathbf{D}\tilde{\mathbf{v}} \tag{2}$$

$$\mathbf{M}\frac{\bar{\mathbf{v}}_{n+1}-\tilde{\mathbf{v}}}{\Delta t}+\mathbf{G}\left(\bar{p}_{n+1}-\bar{p}_n\right)=0 \tag{3}$$

where $\mathbf{M}$ is the mass matrix, $\mathbf{D}$ and $\mathbf{G}$ are the divergence and gradient matrices, $\mathbf{L}$ is the Laplacian and $\mathbf{S}$ is the stabilization matrix, chosen according to [6].

Eulerian formulation for a compressible sub-sonic flow We restrict our model to the sub-sonic regime, thus using the non-conservation form of the governing equations as the basis of the model. Absence of the shock waves in sub-sonic regime permits us this choice. From the impmenetation point of view, the non-conservation form allows to modify the existing incompressible code into a sub-sonic one in a clear and straight-forward manner.

The Navier-Stokes equations written for the compressible fluid consist of momentum, energy, continuity and state equation that read:

$$\rho\frac{\partial \mathbf{v}}{\partial t} - \nabla\cdot\boldsymbol{\sigma} + \rho\left(\mathbf{v}\cdot\nabla\right)\mathbf{v} = \rho\mathbf{b} \tag{4}$$

$$\frac{\partial \rho}{\partial t} + \rho\nabla\cdot\mathbf{v} + \mathbf{v}\cdot\nabla\rho = 0 \tag{5}$$

$$\rho c_v\frac{DT}{Dt} + p\nabla\cdot\mathbf{v} = \nabla\cdot\left(k\nabla T\right) + \Psi + Q \tag{6}$$

$$\rho = \frac{p}{RT} \tag{7}$$

The presence of variable density in the energy equation couples it to the rest of the system [7]. We propose here to integrate the energy equation explicitly, thus decoupling it from the rest of the system. The application of e.g. Forward Euler scheme leads to the following residual form of the energy equation

$$\bar{\mathbf{R}}_e = c_v\mathbf{M}\frac{\bar{T}_{n+1}-\bar{T}_n}{\Delta t} - \left(\mathbf{C}_{(\bar{\mathbf{v}}_n)}\bar{T}_n + R\mathbf{D}_{(\bar{T}_n)}\bar{\mathbf{v}}_n - kL_{(1/\bar{\rho}_n)}\bar{T}_n\right) \tag{8}$$

where $\mathbf{M}$ is the mass matrix, $\mathbf{C}$ is the convective operator and $\mathbf{L}$ is the Laplacian.

The remaining momentum/continuity system is treated using a modified Runge-Kutta time integration scheme in conjunction with the fractional step method [8], [5].

The final discrete momentum/continuity system reads:

$$\mathbf{M}\frac{\tilde{\mathbf{v}}-\bar{\mathbf{v}}_n}{\Delta t} = \frac{1}{6}[\tilde{\mathbf{r}}_1(\bar{\mathbf{v}}_n) + 2\tilde{\mathbf{r}}_2(\bar{\mathbf{v}}_{\beta 1}) + 2\tilde{\mathbf{r}}_3(\bar{\mathbf{v}}_{\beta 2}) + \tilde{\mathbf{r}}_4(\bar{\mathbf{v}}_{\beta 3})] + \mathbf{G}_{(1/\bar{\rho}_n)}\bar{p}_n \tag{9}$$

$$\begin{aligned}\frac{1}{2}\mathbf{L}_{(\rho_n)}\left(\bar{p}_{n+1}-\bar{p}_n\right) + \frac{1}{R\Delta t}\mathbf{M}_{(1/\bar{T}_{n+1})}\bar{p}_{n+1} + \mathbf{C}_{(\tilde{\mathbf{v}}/\bar{T}_{n+1})}\bar{p}_{n+1}) = \\ = \frac{1}{\Delta t}\mathbf{M}\bar{\rho}_n + \mathbf{L}_{(\bar{\rho}_n)}\left(\bar{\rho}_{n+1}R\bar{T}_{n+1}\right)\end{aligned} \tag{10}$$

$$\mathbf{M}\frac{\bar{\mathbf{v}}_{n+1}-\tilde{\mathbf{v}}}{\Delta t} + \frac{1}{2}\left(\mathbf{G}_{(1/\bar{\rho}_{n+1})}\bar{p}_{n+1} - \mathbf{G}_{(1/\bar{\rho}_n)}\bar{p}_n\right) = 0 \tag{11}$$

where the residua $\mathbf{r}_i$ and intermediate fractional velocities are defined as

$$\tilde{\mathbf{r}}_1 = \mathbf{F} - \bar{\mathbf{K}}_{\bar{\mathbf{v}}_n}\bar{\mathbf{v}}_n - \mu\mathbf{L}_{(1/\bar{\rho}_n)}\bar{\mathbf{v}}_n \tag{12}$$

$$\tilde{\mathbf{v}}_{\beta 1} = \bar{\mathbf{v}}_n + \mathbf{M}^{-1}\frac{\Delta t}{2}\tilde{\mathbf{r}}_1 \tag{13}$$

$$\tilde{\mathbf{r}}_2 = \mathbf{F} - \bar{\mathbf{K}}_{\tilde{\mathbf{v}}_{\beta 1}}\tilde{\mathbf{v}}_{\beta 1} - \mu\mathbf{L}_{(1/\bar{\rho}_n)}\tilde{\mathbf{v}}_{\beta 1} \tag{14}$$

$$\tilde{\mathbf{v}}_{\beta 2} = \bar{\mathbf{v}}_n + \mathbf{M}^{-1}\frac{\Delta t}{2}\tilde{\mathbf{r}}_2 \tag{15}$$

$$\tilde{\mathbf{r}}_3 = \mathbf{F} - \bar{\mathbf{K}}_{\tilde{\mathbf{v}}_{\beta 2}}\tilde{\mathbf{v}}_{\beta 2} - \mu\mathbf{L}_{(1/\bar{\rho}_n)}\tilde{\mathbf{v}}_{\beta 2} \tag{16}$$

$$\tilde{\mathbf{v}}_{\beta 3} = \bar{\mathbf{v}}_n + \mathbf{M}^{-1}\Delta t\tilde{\mathbf{r}}_3 \tag{17}$$

$$\tilde{\mathbf{r}}_4 = \mathbf{F} - \bar{\mathbf{K}}_{\tilde{\mathbf{v}}_{\beta 3}}\tilde{\mathbf{v}}_{\beta 3} - \mu\mathbf{L}_{(1/\bar{\rho}_n)}\tilde{\mathbf{v}}_{\beta 3} \tag{18}$$

$$\tag{19}$$

Solution algorithm At this point we can summarize the obtained results in the algorithm of Table 1:

1. Solve the energy equation explicitly and obtain the temperature $\bar{T}_{n+1} = f(\bar{\mathbf{v}}_n, \bar{\rho}_n, \bar{T}_n)$
2. Solve the fractional momentum equation , obtain $\tilde{\mathbf{v}}$ (using $\bar{\rho} = \bar{\rho}_n$ for all the intermediate steps)
3. Solve the continuity equation for the pressure , obtain $\bar{p}_{n+1}$
4. Obtain $\bar{\rho}_{n+1}$ from the ideal gas (state) equation
5. Solve for end-of-step momentum and obtain $\bar{\mathbf{v}}_{n+1}$

Table 1: Implementation of the compressible subsonic flow solver using an explicit solution of the energy equation

2 Examples

Here we present an example for validating the entire (thermo-mechanical) coupling. We choose the heated cavity example, similar to the one addressed in **Chapter 4**. The properties of the heated cavity domain are as follows:

- heat capacity 1000 $[J/kg \cdot K]$
- conductivity 25 $[W/K \cdot m]$
- viscosity 0.001 $[Pa \cdot s]$
- initial temperature 300 $[K]$
- density 1 $[kg/m^3]$
- gravity 10 $[m/s^2]$

At the vertical walls of the cavity the temperatures of 305 [K] and 295 [K] are prescribed.

Here additionally a circular object, placed at $t = 0$ at the center of square domain is subjected to a prescribed motion:

$$\mathbf{u} = 0.05 \cdot sin(5 \cdot t) \tag{20}$$

The circular object has following thermal properties:

- heat capacity 10 $[J/kg \cdot K]$
- conductivity 1000 $[W/K \cdot m]$

We next compare the solution obtained using the Eulerian-Lagrangian strategy derived here with the one obtained using body-fitting ALE approach incompressible fractional-step based formulation (OSS-stabilized). In both cases Boussinesq modification of gravity term is taken into account.

Fig. 1 and 2 show the temperature and velocity contours obtained by both methods at time instances $t = 1.4[s]$ and $t = 15[s]$, corresponding to transitory stage and the periodic stage, when the temperature field is fully developed and the changes in the velocity field occur primarily due to the moving object.

One can see a good agreement between the corresponding distributions.

Remark In this example the comparison was carried out with the ALE formulation. Off course the possibility to treat the interaction "exactly" in the sense of the position of interface and interface boundary conditions is of great advantage. However slightly exceeding the maximum displacement in the present example leads to failure of ALE solver due to mesh deformation, while the proposed methodology allows us to treat arbitrarily large motions of the cylinder or Lagrangian object in general.

Post-processing As we see, in the Eulerian-Lagrangian approach, the fictitious part of the Eulerian domain is disabled. This corresponds to the physical reality. From the point of view of the visualization, it would be very useful to be able to visualize the moving cylinder (Lagrangian part) in the same output file. This is a feature that is lacking by now.

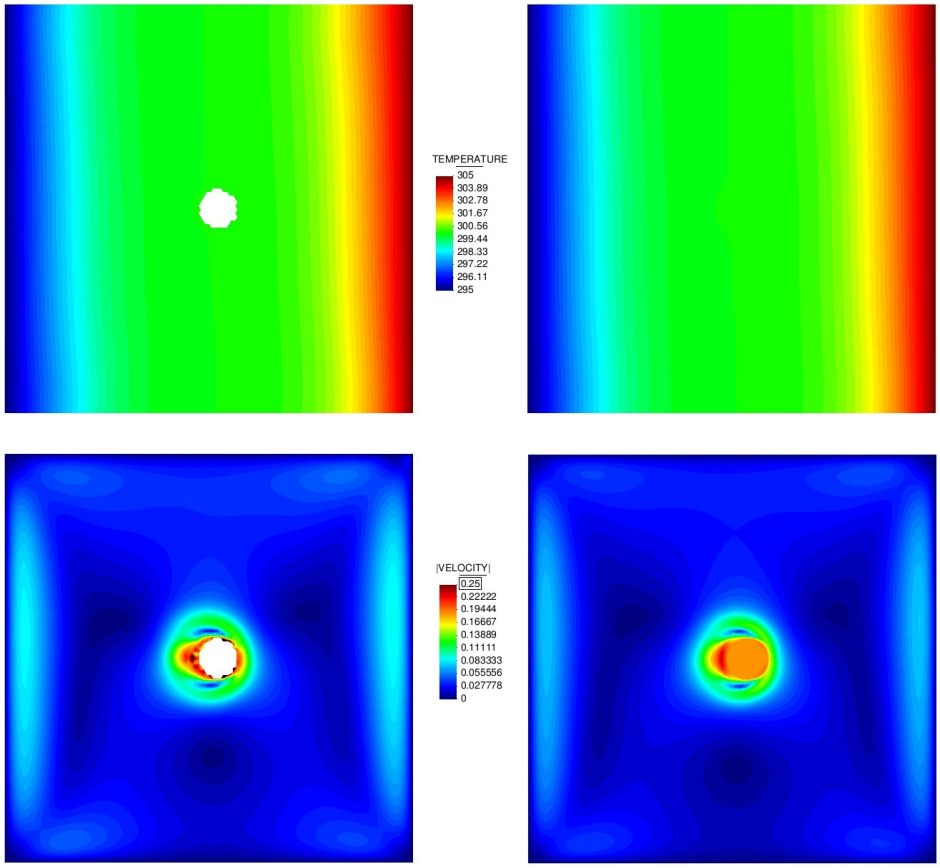

Figure 1: Temperature and velocity contours at t=1.4 [s]: comparison of ALE and Eulerian-Lagrangian coupling

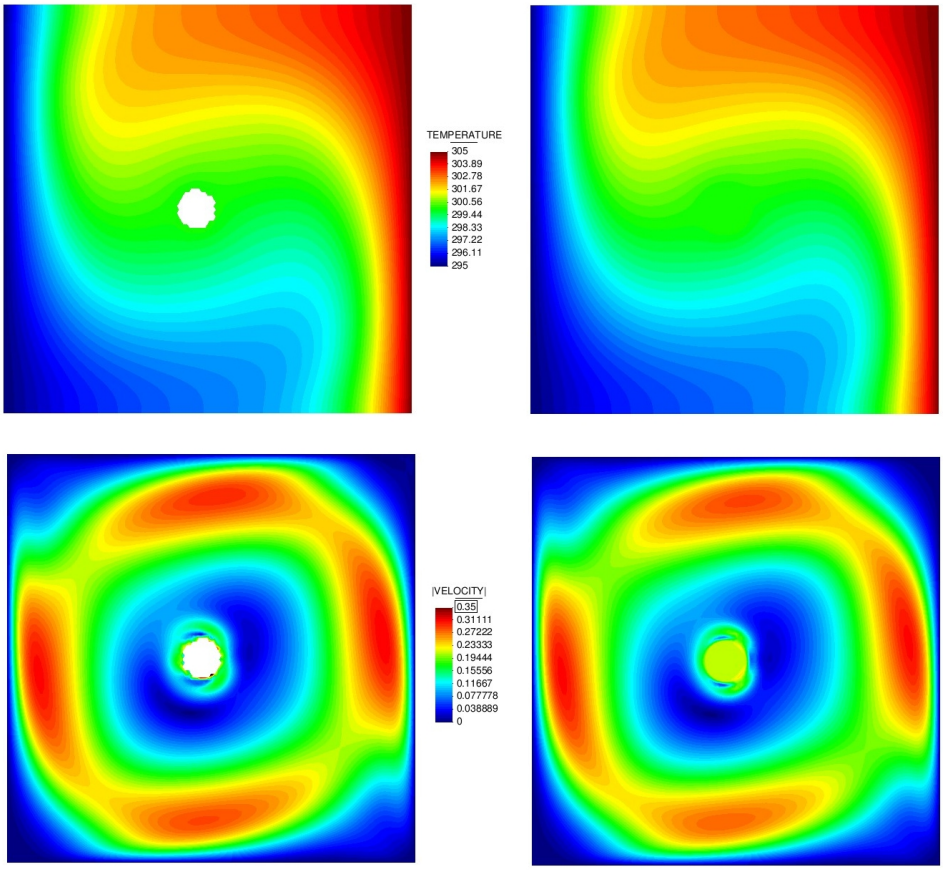

Figure 2: Temperature and velocity contours at t=1.4 [s]: comparison of ALE and Eulerian-Lagrangian coupling

References

[1] Gerstenberger A. and Wall W. An extended finite element/lagrange multiplier based approach for fluid-structure interaction. *Computer Methods in Applied Mechanics and Engineering*, 197:1699–1714, 2008.

[2] Legay A., Chessa J., and Belytschko T. An eulerian-lagrangian method for fluid-structure interaction based on level-sets. *International Journal for Numerical Methods in Engineering*, 195:2070–2087, 2006.

[3] Oñate E., Idelsohn S., Del Pin F., and Aubry R. The particle finite element method: an overview. *International Journal of Computational Methods*, 1:267–307, 2004.

[4] Rossi R., Ryzhakov P., and Oñate E. A monolithic fe formulation for the analysis of membranes in fluids. *Spatial structures*, 24(4):205–210, 2009.

[5] Blair Perot J. An analysis of the fractional step method. *Journal of Computational Physics*, 108:51–58, 1993.

[6] Oñate E. A stabilized finite element method for incompressible viscous. *Comp. Meth. Appl. Mech. Eng.*, 182 (1-2):355–370, 2000.

[7] Codina R., Vazquez M., and Zienkiewizc O.C. A general algorithm for compressible and incompressible flows. *International Journal for Numerical Methods in Fluids*, 27:13–32, 1998.

[8] Codina R. Pressure stability in fractional step finite element method for incompressible flows. *Journal of Computational Physics*, 170:112–140, 2001.